A ROBUST ALGORITHM FOR CORRECTING THE TOPOGRAPHIC EFFECT OF SATELLITE IMAGE OVER MOUNTAINOUS TERRAIN

C.H. Liu
Researcher, Energy & Resources Laboratories, Industrial Technoloy Research Institute, Chutung Hsinchu, Taiwan, R.O.C.

A.J. Chen and G.R. Liu
Professor, Center for Space and Remote Sensing Research, National Central Unverisity, Chung-Li, Taiwan, R.O.C.

Commission 7, Working Group 1

Keywords: Topographic Effect, Digital Terrain Model, Atmospheric Correction Model, Reflectance, SPOT, Classification

ABSTRACT

In order to correct the topographic effect of satellite image over mountainous terrain, a robust algorithm is developed in the atmospheric correction model. Optimized aerosol optical depth is retrieved in the robust algorithm by minimizing the variation of surface reflectances of a selected canopy over different terrains including altitudes, slopes and incidence angles. Digital count image is converted to surface reflectance image by using the atmospheric correction model and digital terrain model. A SPOT image in rugged terrain is used to verify the algorithm. Hardwood is selected in the robust algorithm. For both of hardwood and acacia canopies, difference of reflectances located in shaded and well-illuminated areas are greately reduced, especially in near-IR band after atmospheric correction. Five classes such as forest, high-reflective land, bare soil, urban and grass are well classified with topographic-corrected image by clustering algorithm, whereas uncorrected image classifies terrain related classes such as forest under low and high illumination. The overall accuracy is 91.7%. Kappa statistics is 0.87. It is concluded that classification accuracy is improved by the proposed algorithm.

1. INTRODUCTION

Many applications of remotely sensed data, such as land cover monitoring (Jones *et al.* 1988), crown closure and timber volume estimation (Schieh 1992), and forest damage assessment (Ekstrand 1996), have been hampered due to the topographic effect, which is caused by the differential sensor response to diverse slope and aspect even for a given canopy (Holben and Justice 1980). It is particularly important to correct the topographic effect of satellite image in Taiwan, as two thirds of the land are mountainous areas (Chen and Chen 1991).

Statistical transformations such as band ratio (Holben and Justice 1981), hyperspherical directional cosine (HSDC) (Pouch and Campagna 1990) and principal component (Conese *et al.* 1993a) would lose some informations, although they had yielded good results (Conese *et al.* 1993b). Scene dependent regressed coefficients by combination of DTM in correction of topographic effect (Civco 1989, Colby 1991, Naugle and Lashlee 1992) are also the main obstacle in multi-temporal applications (Conese *et al.* 1993b).

To correct the topographic effect in a deterministic way, an atmospheric correction model is necessary (Conese *et al.* 1993b). Usage of surface reflectance images will not only improve the classification accuracy but also detect the land cover changes in multi-temporal analysis (Kusaka *et al.* 1984). Digital terrain model (DTM) could be combined in the model to delineate the topographic effect of the image. Even for well-illuminated areas, the diffuse irradiance cannot be neglected even though the topographic effect is mainly caused by the beam irradiance (Proy et al. 1989). That is why some developed models (Pons and Sole-Sugranes 1994, Senoo *et al.* 1990) are not suitable for shadow and near shadow areas. Large error such as overcorrection will appear in these areas, if the diffuse irradiance is underestimated. The reflected irradiance by adjacent slope should also be considered in near-IR band if the terrain surrounding is full of vegetation (Proy et al. 1989).

Aerosol optical depth should be obtained before determining diffuse irradiance. Since the diffuse irradiance dominates the global incidence irradiance in shadow, more accurate aerosol optical depth is needed than it does in the flat terrain. Image-based algorithm is desired in operation. As the NDVI of raw image exhibits good correlation with topographic effect, dense dark vegetation (DDV) algorithm developed by Kaufman and Sendra (1988) is not applicable to retrieve aerosol optical depth in rugged terrain (Liu 1995). By the same token, the image-based retrieval algorithm of aerosol characteristics recently developed by the authors (Liu *et al.* 1996) is also not appropriate for the rugged terrain.

The objective of this paper is to modify the atmospheric correction model previous developed (Liu *et al.* 1996) to correct the topographic effect of satellite image. DTM is combined into the model to account for altitude dependent transmittance, terrain related irradiances, such as beam, diffuse and adjacent slope reflected. To map the surface reflectance even in the shadow, optimized aerosol optical depth is retrieved by a proposed robust algorithm such that minimizing the variance of spectral reflectances of pixels at distinct slopes, altitudes and illuminations including shadow for a given canopy. A SPOT image is used to testify the atmospheric correction model. Spectral reflectances of canopies at shadow and well-illuminated area are compared before and after correction. Classification results are also used to verify the method.

2. ATMOSPHERIC CORRECTION MODEL AND THE ROBUST ALGORITHM

Suppose the surface is non-uniform and Lambertian. The atmosphere is assumed to be horizontally stratified. Satellite

remotely sensed radiance L is described by the summation of (1) the atmospheric path radiance L_p, (2) the directly transmitted radiance reflected by the surface L_r, and (3) the scattered radiance by the local environment L_e.

L_r, L_e can be written as:

$$L_r = \frac{E^*_g}{\pi} \rho e^{-\tau/\mu_v} T_g(\mu_v), \quad (1)$$

$$L_e = \frac{E^*_g}{\pi} < \rho > t_d(\mu_v) T_g(\mu_v), \quad (2)$$

where E^*_g is the global irradiance at the inclined surface, ρ and $<\rho>$ are the target and averaged environment reflectance, τ is the sum of Rayleigh and aerosol optical depth, $e^{-\tau/\mu v}$ and $t_d(\mu_v)$ are upward direct and diffuse transmittances respectively due to scattering of molecules and aerosols, $T_g(\mu_v)$ is upward atmospheric transmittance due to gas absorption like O3 , H2O, CO2 and O2 etc., and μ_v is the cosine of viewing zenith angle.

The global irradiance E^*_g is the sum of beam irradiance E^*_b, diffuse irradiance E^*_d, adjacent slope reflected irradiance E^*_{ad} and the irradiance E^*_m due to multiple reflection between atmosphere and ground. E^*_b is expressed by:

$$E^*_b = S_d \mu_I E_s e^{-\tau/\mu_s} T_g(\mu_s), \quad (3)$$

where S_d is the cast-shadow function which is binary, say 0/1 if the direct path between the sun and the target is/isn't intercepted by the surrounding terrain (Proy *et al.* 1989). μ_I is the cosine of incidence angle I between the solar direction and surface normal. E_s is the earth/sun distance-corrected exoatmospheric irradiance (Moran *et al.* 1992). μ_s is the cosine of solar zenith angle. $e^{-\tau/\mu s}$ and $T_g(\mu_s)$ are the same as equation (1) except for downward path.

In determining diffuse irradiance E^*_d, Hay's model is used (Hay 1979, Hay and McKay 1985, Hay *et al.* 1986, Iqbal 1983):

$$E^*_d = E_d\left[\eta\mu_I / \mu_s + 0.5(1-\eta)(1+\cos s)\right], \quad (4)$$

where E_d is the diffuse irradiance for horizontal surface. η is the anisotropy index which defines as the ratio of beam irradiance at the horizontal surface E_b to E_s. As it accounts for the anisotropic distribution of diffuse radiation (Conese *et al.* 1993b), Hay's model is better than the isotropic model (Kondratyev 1977) adopted by some researchers, e.g. Yang and Vidal (1990). s is the slope of the terrain.

E^*_{ad} and E^*_m are expressed respectively by (Iqbal 1983, Duguay and LeDrew 1992):

$$E^*_{ad} = 0.5 < \rho > (E^*_b + E^*_d)(1-\cos s), \quad (5)$$

$$E^*_m = \frac{(E^*_b + E^*_d + E^*_{ad})}{1 - < \rho > r_s} < \rho > r_s, \quad (6)$$

where r_s is the spherical albedo of the atmosphere.

After combining equations (1)~(6), the satellite remotely sensed radiance L is written as:

$$L = \left\{L_p + \mu_s E_s\left\{S_d(\mu_I/\mu_s)e^{-\tau_r/\mu_s} + t_d(\mu_s)\left[\eta(\mu_I/\mu_s) + 0.5(1-\eta)(1+\cos s)\right]\right\} \bullet \left[1 + 0.5 < \rho > (1-\cos s)\right]\left[\rho e^{-\tau/\mu_v} + < \rho > t_d(\mu_v)\right] / \left[\pi(1 - < \rho > r_s)\right]\right\} T_g(\mu_s) T_g(\mu_v), \quad (7)$$

where $t_d(\mu)$ and r_s can be approximated by Eddington method (Liu *et al.* 1996).

Path radiance L_p is also determined as the sum of molecular and aerosol path radiances as in the previous study (Liu *et al.* 1996). The altitude-dependences of molecular optical depths, such as Rayleigh, O3, H2O and uniform gas, are determined by firstly calculating from LOWTRAN 7 (Kneiyzs *et al.* 1988) with radiosonde data and then being well regressed to be exponential decay model.

Before determining surface reflectance ρ, uniform target is assumed, i.e. $<\rho> = \rho = \rho_0$. Equation (7) is then written as:

$$L = \left\{L_p + \mu_s E_s\left\{S_d(\mu_I/\mu_s)e^{-\tau/\mu_s} + t_d(\mu_s)\left[\eta(\mu_I/\mu_s) + 0.5(1-\eta)(1+\cos s)\right]\right\} \bullet \left[1 + 0.5\rho_0(1-\cos s)\right]\rho_0\left[e^{-\tau/\mu_v} + t_d(\mu_v)\right] / \left[\pi(1-\rho_0 r_s)\right]\right\} T_g(\mu_s) T_g(\mu_v), \quad (8)$$

From above equation, one can see remotely sensed radiance L is a function of reflectance ρ_0, altitude z, slope s, shaded reflief $S_d\mu_I$ and atmospheric parameters. z and s can be determined for a given terrain, such as digital terrain model (DTM). $S_d\mu_I$ can also be determined from the given terrain and solar geometry for a specific image. The molecular optical depths can be computed from the regressed equation with known radiosonde data. The left unknowns are then ρ_0 as well as the aerosol characteristics, i.e. single scattering albedo ω_o, scattering phase function $P_a(\Theta)$ and optical depth τ_a which are implicit in equation (8).

Junge size distribution is assumed as in the previously developed atmospheric correction model of horizontal surface (Liu *et al.* 1996). It should be emphasized that the Junge parameter v is assumed to be a mean value 3.3 (Iqbal, 1983) in the following proposed robust algorithm, whereas it can be iteratively retrieved from the image itself based on DDV by the image-based iterative algorithm in the flat surface (Liu *et al.* 1996). The reason why we didn't use DDV to retrieve aerosol characteristics is that NDVI image determined from raw image of a rugged terrain demonstrated highly correlated with the topography (Liu 1995). In this study, the aerosol type is assumed to be continental. The radius size ranges from

[0.01 ~ 10]μm. Then ω_o and $P_a(\Theta)$ can be determined from the Mie theory.

Here we propose the robust algorithm to retrieve aerosol optical depth from the image itself. One can select pixels of a given canopy with different altitude z, slope s and incidence angle I from the ancillary data, such as airphoto, base map and DTM. The merit function is defined as the ratio of standard deviation to average of derived surface reflectances of those selected pixels. By minimizing the merit function such as Powell minimization method (Press *et al.* 1992), optimized aerosol optical depth can be determined. The algorithm is so-called "robust" because of its robustness. Certainly, the algorithm is limited by the a-priori knowledge of the geographic coordinates of the selected canopy. The dynamic range of the selected pixels also limits the application of the robust algorithm.

The altitude-dependent aerosol optical depth is modeled as $\tau_a=\tau_{ao}-c_o z$, where τ_{ao}, c_o are the sea-level optical depth and the linear decay rate (km^{-1}). In this study, the variance of surface reflectances of selected pixels in robust algorithm is too large, if one use exponential decay model of aerosol. It is also noted that the altitude-dependent aerosol optical depth shows linear decrease from simulation study of LOWTRAN 7 (Liu 1995).

After knowing ω_o and $P_a(\Theta)$, ρ_0 and optical depth τ_a are the left unknowns in equation (8). The optimized τ_{ao} and c_o can be retrieved by using the proposed robust algorithm. Penalty function suggested by Liang and Strahler (1994) is added in the merit function in order to force the retrieved τ_{ao} and c_o to fall in the reasonable ranges which can be determined from LOWTRAN 7 with reasonable visibility ranges 5~336 km (Liu 1995). After ω_o , $P_a(\Theta)$ are assumed and the initial guesses of τ_{ao} and c_o are given, the four dimensional look-up table $L=L(\rho_o, z, s, S_d\mu_l)$ is built up. Then, every ρ_o of the selected pixels in the robust algorithm is determined from the interpolation of the above look-up table with known z, s, $S_d\mu_l$ and L. The optimized τ_{ao} and c_o are finally iteratively retrieved by minimizing the variation of reflectances of the selected pixels. The retrieved ones are so called "optimized" because those deviated values from the optimized ones would result in larger variation of the reflectances of the selected canopy (see section 4). And then ρ_o image of the topographic-effect corrected can be generated by the optimzed aerosol optical depth and the look-up table.

By comparing equation (7) and equation (8), one can obtains the remotely sensed ground reflectance ρ which can be written as:

$$\rho=\begin{cases}\rho_0 & \left[1+0.5\rho_0(1-\cos s)\right]\left[e^{-\tau/\mu_v}+t_d(\mu_v)\right] \\ & \left[1+0.5\langle\rho\rangle(1-\cos s)\right] \end{cases} \Bigg| \begin{cases} & 1-\langle\rho\rangle r_s \\ & 1-\rho_0 r_s \end{cases} - \langle\rho\rangle t_d(\mu_v) \Bigg\} / e^{-\tau/\mu_v}, \quad (9)$$

where $\langle\rho\rangle$ is simply determined by averaging ρ_o of the local window (Richter ,1990). The window size is selected to be about 1 km which is the same as the previous study (Liu *et al.* 1996). If the terrrain is flat, i.e. s=0 , equation (9) will be certainly reduced to be equation (15) of Liu *et al.* (1996).

3. DATA DESCRIPTION

The test site is located in Taoyuan county, northern Taiwan and is about 7.5km×7.5km. The altitudes range from 100~400m. The slopes range from 0°~49° with mean slope 12°. The area is covered mainly by hardwoods, acacia, tea, grassland, bare soil, high-reflective land and urban.

A SPOT image taken on 30 December 1993 is used to testify the algorithm. Its apparent reflectance image is shown in Fig. 1a. The solar and viewing zenith angles are 51.9° and 15.8° respectively. The relative azimuth angle is 53°.

DTM provided by Aerial Survey Institute with 40m spatial resolution is resampled to correspond with that of satellite image by using cubic convolution method (Kawata *et al.* 1988). DTM is firstly gaussian-filtered to remove much of noise (Seemuller 1989). Slope s and aspect a are then determined by the following equations with two partial derivatives computed by the third-order finite difference method (Skidmore 1989):

$$[\partial z/\partial x]_{i,j}=[(z_{i+1,j+1})+2(z_{i+1,j})+(z_{i+1,j-1})] - [(z_{i-1,j+1})+2(z_{i-1,j})+(z_{i-1,j-1})]/8\Delta x, \quad (10)$$

$$[\partial z/\partial y]_{i,j}=[(z_{i+1,j+1})+2(z_{i,j+1})+(z_{i-1,j+1})] - [(z_{i+1,j-1})+2(z_{i,j-1})+(z_{i-1,j-1})]/8\Delta y, \quad (11)$$

$$\tan s = \sqrt{\left[(\partial z/\partial x)^2 + (\partial z/\partial y)^2\right]} \quad (12)$$

$$\tan a = \frac{(\partial z/\partial x)}{(\partial z/\partial y)}. \quad (13)$$

The incidence angle I of beam irradiance is computed as follows (Duguay and LeDrew 1992):

$$I = \cos^{-1}\left(\cos\theta_s \cos s + \sin\theta_s \sin s \cos(a-\phi_s)\right), \quad (14)$$

where θ_s, ϕ_s are solar zenith and azimuth angles respectively. Ray tracing method is applied to determine cast-shadow function S_d (Proy *et al.* 1989). Fig. 2 shows the shaded relief $S_d\mu_l$ image determined from DTM data and corresponded to the solar geometry at the time of the SPOT overpass.

4. RESULTS AND DISCUSSIONS

To account for the altitude dependence of the molecular scattering and absorption, radiosonde data of the Panchiao city located from about 40km is used as inputs of LOWTRAN 7.

The robust algorithm is applied to retrieve the optimized aerosol optical depth. In this study, pixels of hardwood are selected carefully by the base maps. To avoid mixed pixel, central pixel of homogeneous slope is selected. The dynamic ranges

of altitude z, slope s and shaded relief $S_d\mu_l$ of these pixels are 170~290m, 12^0~41^0 and 0.0~0.9 respectively. Owing to the topographic effect, the digital counts of the hardwood canopy varies from 34~40, 29~36 and 24~66 in XS1, XS2 and XS3 bands respectively (Fig. 2). That such large variation of sensor response of a given canopy , especially in XS3 band, is the main reason to hamper the application of satellite image over mountainous terrain. The retrieved sea-level aerosol optical depth τ_{a0} (underline) are 0.46, 0.37, 0.44 and linear decay rate c_o are 0.091, 0.071, 0.001 in XS1~XS3 bands respectively (Table 1). Mean hardwood reflectances μ are 0.026, 0.023 and 0.206 respectively in XS1~XS3 bands respectively. Sensitivity of derived surface reflectance to aerosol optical depth is also studied by artificially deviating the optimized τ_{a0} to ± 0.1. When τ_{a0} is under-estimated 0.1, μ is over-estimated up to 0.049, 0.053 and 0.232 in XS1~XS3 bands respectively. On the contrary, μ is under-estimated to 0.186 in XS3 band and even negative value ('fail' denoted in Table 1) in XS1 and XS2 bands respectively. When τ_{a0} is deviated, surface reflectance at nearby shadow ($S_d\mu_l \rightarrow 0.0$) is more sensitive to aersol optical depth than that at well illuminated as shown in Fig. 3. This is because diffuse irradiance determined from aerosol optical depth is dominated in nearby shadow terrain. The error of derived reflectance at shadow in rugged terrain can be up to 0.1 in XS1~XS3 bands when $\Delta\tau_{a0}$ is 0.1, whereas the error is only about 0.01 in horizontal surface (Liu *et al.* 1996). Thus it could be concluded that more accurate aerosol optical depth should be needed in rugged terrain, if equal accuracy of surface reflectance is required. It is also noted that the optimized τ_{a0}s in XS bands don't follow Angstrom formula. τ_{a0} in XS3 band is greater than that in XS2 band. Probably it results from: (1) Lambertian surface assumption of the atmospheric correction model; (2) inaccurate modeling of adjacent slope reflected irradiance E^*_{ad}.

The surface reflectance is derived by correcting the atmospheric and topographic effects of the image. Table 2 shows the difference of mean reflectance in shaded and wel-illuminated (μ_l>0.8) terrain before and after atmospheric correction. Acacia is chosen to verify the result of correction and testify the sensitivity of the algorithm to selected canopy. Typical spectral reflectances demonstrate the effect of atmospheric correction. In addition, difference of reflectances of pixels located in shaded and well-illuminated areas are greately reduced, especially in near-IR band. The reflectance difference of acacia in shade and well-illuminated area is -0.024 in XS3 band, which is largely compared to the hardwood (-0.001) selected to retrieve the aerosol optical depth in the robust algorithm. Thus the algorithm is considered to be sensitive to the selected canopy. It is again probably due to the insufficiency of Lambertian surface assumption.

By using the atmospheric correction model with retrieved aerosol optical depth as input, topographic effect is largely corrected in surface reflectance image (Fig. 1b) as compared to apparent reflectance image (Fig. 1a). To view the difference between with and without correction, the same enhancement function is applied. However, there are still some pixels under-corrected or over-corrected both at ridge or valley and intersection of bright-dark area. It is due to insufficiency of DTM spatial resolution or resampling of geometric correction in such a drastic change terrain. Landcover change may be one of the reasons as shown in the lower-left part of Fig. 1b. This area is over-corrected because its shaded relief (Fig. 2) is under-estimated.

Classification results bewteen with and without correction are also used to testify the algorithm. ISOCLASS clustering algorithm (IDIMS, 1992) is applied in classification. Uncorrected image is clustered to classes of urban, high-reflective land, mixed bare soil and urban, and two terrain related classes such as forest under high illumination, forest under low illumination (Fig. 4a). These spectral classes didn't correspond with real ground canopies very well, especially two terrain related forest classes due to topographic effect. However, forest, high-reflective land, bare soil, urban and grass are fairly well clustered if one uses the surface reflectance image to classify (Fig. 4b). The forest class includes hardwoods, acacia and tea, because their pairwise transformed divergences are all smaller than 1.6. The overall accuracy is 91.7%. Kappa statistics is 0.87 (Congalton 1991). One can conclude that classification accuracy is improved if the satellite image is corrected by the atmospheric correction model.

5. CONCLUSION

Promising reduction of topographic effect of satellite image is achieved by using the proposed atmospheric correction model. Aerosol optical depth retrieved in the robust algorithm is shown to be optimized as deviated ones can produce large error in shadow areas. In comparing the sensitivity study of the previous study (Liu *et al.* 1996), more accurate aerosol optical depth is needed to determine the surface reflectance in rugged terrain than in flat terrain. Classification accuracy is also improved by the corrected image.

Although the results are rather encouraging, more studies should be undertaken:
(1) verification of the aerosol optical depth by field measurement, and possible testify the model of adjacent slope reflected irradiance;
(2) extension of the atmospheric correction model with non-Lambertian surface;
(3) with DTM spatial resolution comparable to satellite image (Conese *et al.* 1993b), and possible with apparent DTM considering the tree-top of the terrain (Liu 1995, Chen and Rau 1993). This work is undertaken by the authors.

REFERENCES

Chen A.J. and J.Y. Chen, 1991, Using Lowtran6 and DEM to derive surface reflectance factor from SPOT HRV data. *IGARSS'91*,June3-6,Espoo, Finland,pp.651-654.

Chen L.C. and J.Y. Rau, 1993, A unified solution for digital terrain model and orthoimage generation from SPOT stereopairs. *IEEE Trans. on Geos. and Remote Sens.*, vol.31, no.6, pp1243-1252.

Civco D.L., 1989,Topographic normalization of Landsat thematic mapper digital imagery, *Photogramm. Eng. and Remote Sens.*, v55, n9, pp1303-1309.

Colby J.D., 1991, Topographic normalization in rugged terrain, *Photogramm. Eng. and Remote Sens.*,v57, n5, pp531-537.

Conese C., G. Maracchi, and F. Maselli, 1993a, Improvement in maximum likelihood classification performance on highly rugged terrain using principal component analysis,

International Journal of Remote Sensing, vol.14, no.7, pp.1371-1382.

Conese C., M.A. Gilabert, F. Maselli, and L. Bottai, 1993b, Topographic normalization of TM scenes through the use of an atmospheric correction method and digital terrain models. *Photogramm. Eng. and Remote Sens.*, vol.59, no.12, pp1745-1753.

Congalton R.G., 1991, A review of assessing the accuracy of classifications of remotely sensed data, *Remote Sens. Environ.* ,37:35-46.

Duguay C.R. and E.F. LeDrew, 1992, Estimating surface reflectance and albedo from Landsat-5 thematic mapper over rugged terrain, *Photogramm. Eng. Remote Sens.*, v58,n5, pp551-558.

Ekstrand S., 1996, Landsat TM-based forest damage assessment: correction for topographic effect, *Photogrammetric Engineering & Remote Sensing*, vol. 62, no.2, pp.151-161.

Hay J.E., 1979, Calculation of monthly mean solar radiation for horizontal and inclined surfaces. *Solar Energy*, vol.23, pp.301-307.

Hay J.E. and D.C. McKay, 1985, Estimatiing solar irradiance on inclined surfaces: a review and assessment of methdologies. *Int. J. Solar Energy*, vol.3, pp.203-240.

Hay J.E., R. Perez, and D.C. McKay, 1986, Addendum and errata to the paper estimating solar irradiance on inclined surfaces: a review and assessment of methdologies. *Int. J. Solar Energy*, vol.4, pp.321-324.

Holben B.N. and C.O. Justice, 1980, The topographic effect on spectral response from nadir-pointing sensors, *Photogramm. Eng. Remote Sens.*, v46,n9, pp1191-1200.

Holben B.N. and C.O. Justice, 1981, An examination of spectral band ratioing to reduce the topographic effect of remotely sensed data, International Journal of Remote Sensing, vol. 2, pp.115-123.

Iqbal, M., 1983, *An introduction to solar radiation*(Toronto, New York, London: Academic Press), 390pp.

Jones A.R., J.J. Settle, and B.K. Wyatt, 1988, Use of digital terrain data in the interpretation of SPOT-1 HRV multispectral imagery, *Int. J. Remote Sens.*,vol.9, no.4, pp669-682.

Kaufman, Y.J., and Sendra, C., 1988, Algorithm for automatic atmospheric corrections to visible and near-IR satellite imagery, *International Journal of Remote Sensing*, **9**, 1357-1381.

Kawata Y., S. Ueno and T. Kusaka, 1988, Radiometric correction for atmospheric and topographic effects on landsat MSS images, *Int. J. Remote Sens.*, vol.9, no.4, pp729-748.

Kneizys, F.X., Shettle, E.P., Abreu, L.W., et al., 1988, *Users guide to LOWTRAN 7*, Report AFGL-TR-88-0177, Air Force Cambridge Research Laboratories, Bedford, MA, August, 137pp.

Kondratyev K.Y., 1977, Radiation regime of inclined surfaces, Tehnical Note No. 152, World Meteorological Organization, Geneva, No. 467.

Kusaka T., Y. Kawata, and S. Ueno, 1984, Multi-temporal data analysis by extended radiometric correction, Proceedings of the 18th International Symposium on Remote Sensing of Environment (Michigan: ERIM), pp.1775-1783.

Liu C.H., 1995, Radiometric correction of SPOT satellite imagery, Ph.D. dissertation, National Central Univerisity, 217p.

Liu C.H., Chen, A.J., and Liu, G.R., 1996a, An image-based retrieval algorithm of aerosol characteristics and surface reflectance from satellite image. accepted by *International Journal of Remote Sensing*.

Moran, M.S., Jackson, R.D., Slater, P.N., and Teillet, P.M., 1992, Evaluation of simplified procedures for retrieval of land surface reflectance factors from satellite sensor output, *Remote Sensing Environment*, **41**, 169-184.

Naugle B.I. and J.D. Lashlee, 1992, Alleviating topographic influences on land-cover classifications for mobility and combat modeling, *Photogramm. Eng. Remote Sens.*, 58:1217-1221.

Pons x. and L. Sole-Sugranes, 1994, A simple radiometric correction model to improve automatic mapping of vegetation from multispectral satellite data. *Remote Sens. Environ.*, 48:191-204.

Pouch G.W. and D.J. Campagna, 1990, Hyperspherical directional cosine transformation for separation of spectral and illumination information in digital scanner data, *Photogramm. Eng. Remote Sens.*, v56, n4, pp475-479.

Press W.H., S.a. Teukolsky, W.T. Vetterling, and B.P. Flannery, 1992, *Numerical Recipes in Fortran*. Second Edition, 963pp.

Proy C., D. Tranre, and P.Y. Deschamps, 1989, Evaluation of topographic effects in remotely sensed data, *Remote Sens. Environ.*, 30:21-32.

Schieh H.C., 1992, Studies on the application of MSS data in the stand crown-closure and volume estimate of Cryptomeria, Ph.D. disseration, National Taiwan Unverisity, 166p.

Seemuller W.W., 1989, The extraction of ordered vector drainage networks from elevation data, *Computer vision, Graphics and Image Processing* ,47:45-58.

Senoo T., F. Kobayashi, S. Tanaka and t. Sugimura, 1990, Improvement of forest type classification by SPOT HRV with 20m mesh DTM, *Int. J. Remote Sens.*, vol.11, no.6, pp1011-1022.

Skidmore A.K., 1989, A comparison of techniques for calculating gradient and aspect from a gridded digital elevation model. *International Journal of Geographical Information Systems*, vol.3,no.4,pp323-334.

Yang C. and A. Vidal, 1990, Combination of digital elevation models with SPOT-1 HRV multispectral imagery for reflectance factor mapping, *Remote Sens. Environ.*, 32:35-45.

Please regard the colour page with Fig. 1 and Fig. 4 at the end of the volume.

Table 1. Retrieved sea-level aerosol optical depth τ_{a0} and linear decay rate c_o (underline) in different XS bands by the robust algorithm. μ and σ are mean and standard deviation of derived surface reflectances of the selected pixels of hardwood. Also lists sensitivity of μ and σ to τ_{a0}. 'fail' means that it fails to interpolate surface reflectance from the look-up table.

XS	τ_{ao}	c_o	μ	σ	σ/μ
1	0.36	0.091	0.049	0.0218	0.447
	0.46	0.091	0.026	0.0055	0.212
	0.56	0.091	fail	fail	fail
2	0.27	0.071	0.053	0.0333	0.625
	0.37	0.071	0.023	0.0087	0.372
	0.47	0.071	fail	fail	fail
3	0.34	0.001	0.232	0.0418	0.180
	0.44	0.001	0.206	0.0136	0.066
	0.54	0.001	0.186	0.0301	0.162

Table 2. Mean value of apparent and derived surface reflectances in shadow and well-illuminated (μ_I>0.8) terrain for hardwood and acacia in XS bands. Difference mean reflectance of well-illuminated pixel minus that of shaded pixel.

XS	Apparent Reflectance			Surface Reflectance		
	Shade	Well Illum.	Difference	Shade	Well Illum.	Difference
			Hardwood			
1	0.095	0.106	0.011	0.025	0.019	-0.006
2	0.065	0.077	0.012	0.027	0.018	-0.009
3	0.097	0.239	0.142	0.207	0.206	-0.001
			Acacia			
1	0.095	0.104	0.009	0.020	0.017	-0.003
2	0.064	0.073	0.009	0.019	0.016	-0.003
3	0.119	0.250	0.131	0.260	0.236	-0.024

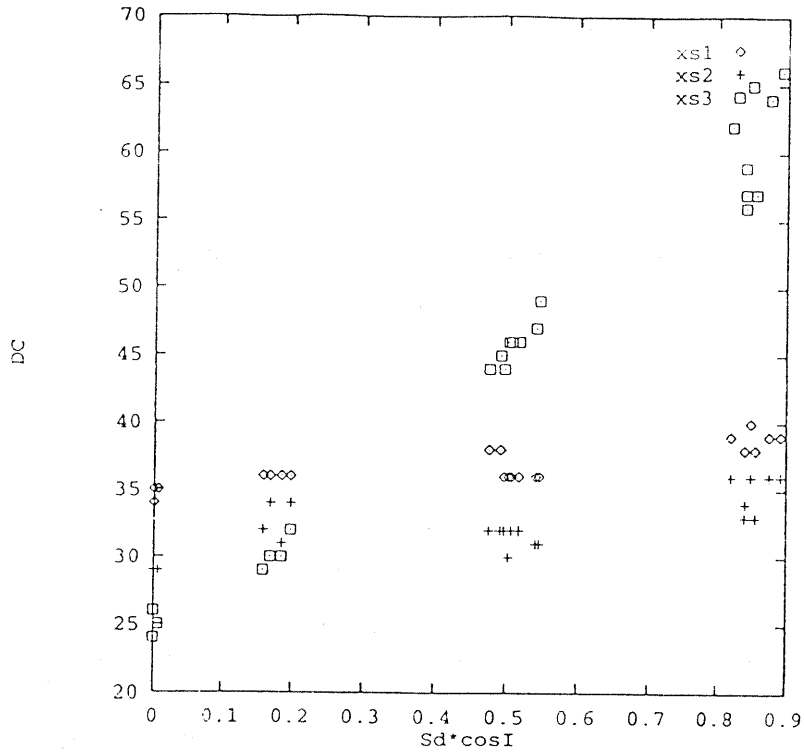

Figure 2. Digital counts of selected hardwood pixels in various shaded relief $S_d\mu_l$ in different XS bands.

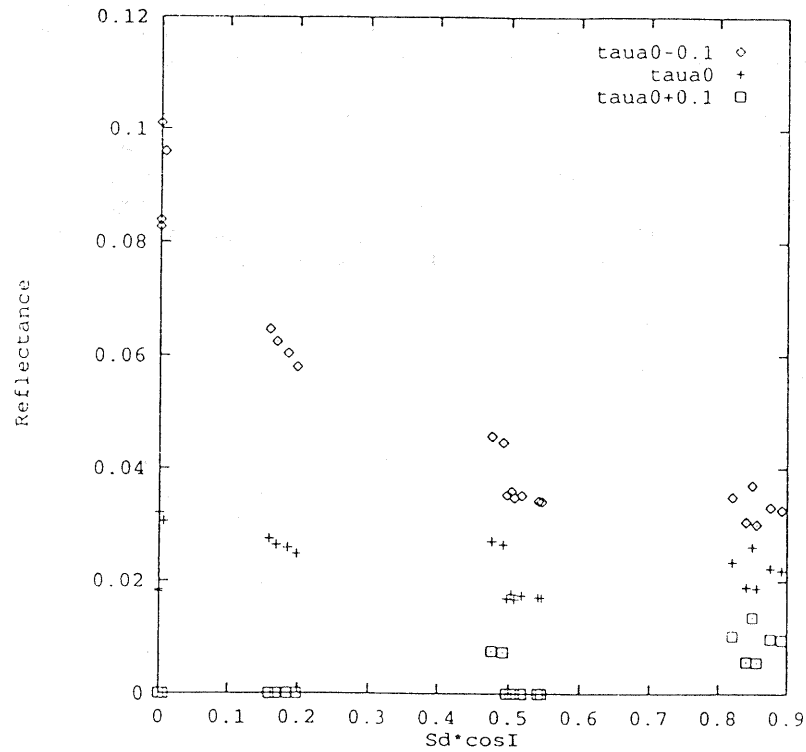

Figure 3. Relationship of hardwood reflectance to shaded relief $S_d\mu_l$ with optimized aerosol optical depth τ_{a0} and $\tau_{a0}\pm0.01$ in XS1 band.